Meteorites
Vol. 1, No. 1, 2011, 29–38
www.meteorites.pwr.wroc.pl
DOI 10.5277/met110104

INVESTIGATIONS OF HAH 286 EUCRITE BY ANALYTICAL ELECTRON MICROSCOPY

Marian SZURGOT[1], Krzysztof POLAŃSKI[2]

[1] Technical University of Łódź, Center of Mathematics and Physics, Al. Politechniki 11, 90 924 Łódź, Poland.
[2] University of Łódź, Department of Solid State Physics, ul. Pomorska 149/153, 90-236 Łódź, Poland.

Abstract: The elemental composition, mineral composition and microstructure of the HaH 286 eucrite found in Lybia in 2000 were studied by analytical electron microscopy. It was established that the mean elemental composition of HaH 286 and atomic and molar ratios: Fe/Mn = 34, Mg/Mg+Fe = 36, Na/Al = 0.066, and Ca/Al = 0.73 are typical of eucrites, and two main meteorite minerals have the mean composition: clinopyroxene En34Fs59Wo7 and plagioclase feldspar An88Ab12. Variations in the composition of pyroxenes and plagioclases are as follows: pyroxene En34-36Fs53-62Wo3-13 and plagioclase: An86-100Ab14-0. Pyroxene is represented by pigeonite and by orthopyroxene. Chromite, ilmenite and silica are minor minerals. The composition, atomic ratios and microstructure indicate that the HaH 286 meteorite is a pyroxene-plagioclase basaltic achondrite, a non-cumulate eucrite with the composition of plagioclase changing between anorthite and bytownite.
Keywords: Eucrite, Hammadah al Hamra 286, analytical electron microscopy, meteorite

INTRODUCTION

Hammadah al Hamra 286 (HaH 286) is one of the Saharan meteorites found in Lybia in 2000. The meteorite was classified as an eucrite in 2001 (Grossman & Zipfel, 2001). Preliminary compositional data for this meteorite are as follows: clinopyroxene Fs28-38Wo32-43, plagioclase An77-92, ferrosilite content 55-60 mol% and shock stage S4 (Grossman & Zipfel, 2001). Studies of thermophysical properties have been recently conducted (Szurgot, 2003, 2011a,b; Szurgot & Wojtatowicz, 2011). Preliminary results of the characterisation of minerals of this HaH meteorite by micro-Raman spectroscopy have been recently published (Szurgot et al., 2011). The aim of this paper is to determine and analyse the elemental and mineral composition of the meteorite and to characterize its microstructure using analytical electron microscopy.

EXPERIMENTAL

The meteorite sample (3g, 32 × 21 × 2.2 mm) was prepared as a polished plate (Fig. 1). The sample was bought from Andrzej Pilski, a well known collector of meteorites. A Tescan VEGA 5135 scanning electron microscope (SEM) and an Axiotech Zeiss optical microscope were used to identify various minerals and to analyze the microstructure and texture of the rock.

The elemental composition of the meteorite was determined by energy dispersive X-ray (EDX) method using an EDX Link 3000 ISIS X-ray microanalyser (Oxford Instruments) with a Si(Li) detector. Oxfords Instruments standards were used for calibration, and a ZAF program was employed for correcting the elemental compositions of minerals. The EDX measurements are accurate to approximately 0.5%.

Elemental X-ray maps of Fe, Al, Ca, Mg, Cr, Si and O were used to create mineral maps and to estimate the modal abundance of the major mineral phas-

Corresponding author: Marian SZURGOT, mszurgot@p.lodz.pl

Fig. 1. Macroscopic view of the HaH 286 meteorite sample. White minerals are plagioclases, gray minerals are pyroxenes.

es – pyroxene and plagioclase, as well as the minor minerals – silica, ilmenite and chromite. The measurement of the relative area occupied by a given mineral, which represents the relative volume of the mineral in the rock, is accurate to roughly 5%.

Back scattered electron (BSE) and optical images of various parts of the meteorite were collected and analyzed. BSE electrons coming from the collimated beam of electrons scattered by the minerals of the sample were collected by YAG scintillator detector. Because the number of counts is directly proportional to the atomic number of the object, the white spots on the image mark the heavy elements, gray spots represent medium elements, and black spots reveal the light elements in the sample (Reed, 2000; Polański, 2008).

RESULTS AND DISCUSSION

Elemental Composition

Figure 2 shows the energy dispersive X-ray spectrum (EDS, EDX spectrum) of the HaH 286 sample and Tab. 1 presents the mean elemental composition of the meteorite. The element content is expressed by weight and atomic percent. A relatively large region of the meteorite (with an area of about 25 mm^2) was irradiated with electrons to generate these X-ray quanta.

Tab. 1 shows that the main chemical components of the meteorite are: Si (21.21 wt%), O (45.18 wt%), Fe (12.80 wt%) and Mg (3.18 wt%), Ca (8.61 wt%), Al (7.89 wt%). They create about 99% of the mass of the minerals constituting the meteorite. Five elements make up remained one percent of the meteorite mass: Na (0.44 wt %), Mn (0.38 wt%), Ti (0.30 wt%), Cr (0.13 wt%) and S (0.1 wt%). Data of Johum and coworkers (Johum et al., 1980) on the elemental composition of the Yamato 74450, Pasamonte and Stannern eucrites are also included in the table. According to the figures, the agreement between our results and

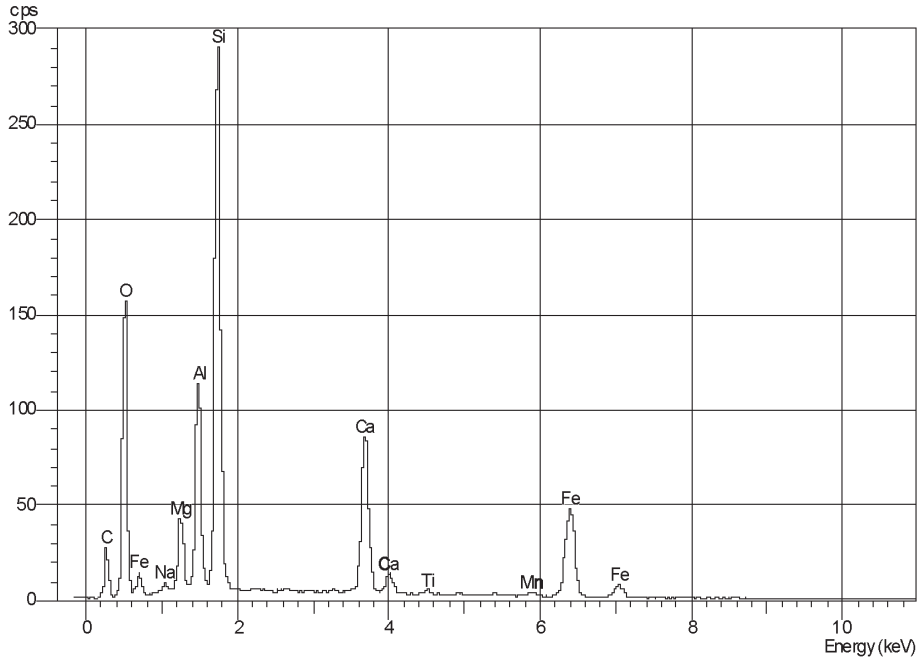

Fig. 2. EDS spectrum of HaH 286 meteorite revealing major elements contributing to the mean bulk composition of the meteorite

Table 1. Mean elemental composition of HaH 286, Yamato 74450, Pasamonte and Stannern eucrites

Element	HaH 286 wt%, (atomic%) (authors own data)	Yamato 74450 wt% (Jochum et al., 1980)	Pasamonte wt% (Jochum et al., 1980)	Stannern wt% (Jochum et al., 1980)
O	45.18 (63.05)	45.5*	44.5*	46.3*
Si	21.21 (16.86)	22.2	23.7	22.5
Mg	3.18 (2.92)	4.2	3.9	4.4
Fe	12.18 (5.12)	13.9	13.4	12.7
S	0.10# (0.07)#	0.13	0.039	0.42
Al	7.89 (6.53)	6.3	6.5	6.0
Ca	8.61 (4.80)	7.0	7.4	7.2
Ni	nd	< 0.04	< 0.04	< 0.04
Na	0.44 (0.43)	0.27	0.31	0.31
Cr	0.13# (0.05)#	0.31	0.14	0.16
Mn	0.38 (0.15)	0.44	0.37	0.33
K	nd	0.041	0.034	0.037
Ti	0.30 (0.14)	ns	ns	ns
Total	100 (100)	100	100	100

*Added to 100 %.

S and Cr content was added since these elements were revealed in another EDS spectrum; nd = not detected, ns = not specified.

literature data for elements present in the HaH 286 meteorite and in eucrites (Jochum et al., 1980; Mittlefehldt et al., 1998; Hutchison, 2004) is satisfactory.

The same conclusion can be drawn from the analysis of atomic ratios for selected elements traditionally used in analyses of eucrites. The Fe/Mn, Ca/Al, Na/Al, mg# = 100 Mg/[Mg+Fe], fe# = 100 Fe/[Mg+Fe], and mg = 100 Mg/[Mg+Fe+Ca] ratios for the HaH 286 meteorite and Y 74450, Pasamonte, and Stannern eucrites are compiled in Tab. 2.

According to the data, Fe/Mn, Ca/Al, Na/Al, mg#, mg, and fe# ratios lie within or close to the range of values established for eucrites (Hutchison, 2004; Mayne et al., 2009; McSween & Huss, 2010, McSween et al., 2011).

Tab. 3 presents the composition of HaH 286 and selected eucrites given by oxide contents (wt %). HaH 286 contains: SiO_2 (46.38%), MgO (5.36%), FeO (16.82%), Al_2O_3 (15.19%), CaO (12.32%), Cr_2O_3 (0.29%), Na_2O (0.51%), MnO (0.49%) and TiO_2 (0.52%). The data show that the mean oxides composition of HaH 286 is within the values exhibited by eucrites (Mason et al., 1979; Johum et al., 1980; Mittlefehldt et al., 1998; Barrat et al., 2000; Hutchison, 2004; Yamaguchi et al., 2009). The MgO content of HaH 286 is somewhat lower, and Al_2O_3 and CaO contents are somewhat higher than in eucrites. S content (0.10 wt%) is of the same order magnitude as in eucrites (0–0.15 wt%), and K_2O and P_2O_5 have not been detected.

The seventh and eighth columns in Tab. 3 indicate that HaH 286 belongs to the basaltic, non-cumulate eucrites (compare TiO_2, Na_2O, and Cr_2O_3 content in HaH 286 with contents of non-cumulate eucrites). The location of the experimental point for HaH 286, TiO_2 content vs. FeO/MgO ratio, in a diagram published by Barrat and coworkers (Barrat et al., 2000), also proves that HaH 286 is a non-cumulate rather than cumulate eucrite. Fig. 3 shows that the location

Table 2. Atomic ratios in HaH 286 and other eucrites

Ratio	HaH 286	Eucrites (Hutchison, 2004)	Yamato 74450 (Jochum et al., 1980)	Pasamonte (Jochum et al., 1980)	Stannern (Jochum et al., 1980)
Fe/Mn	34	30-33	31[1)]	36[1)]	38[1)]
mg#	36	ns	41	40	44
fe#	64	ns	59	60	56
mg	23	ns	29	27	31
Ca/Al	0.73	0.72-0.79	0.75	0.77	0.81
Na/Al	0.066	ns	0.050	0.056	0.061

mg# = 100 Mg/[Mg+Fe]; fe# = 100 Fe/[Mg+Fe]; mg = 100 Mg/[Mg+Fe+Ca].

[1)] Data for Yamato 74450, Pasamonte and Stannern were calculated on the basis of the weight content of elements; ns = not specified.

Table 3. Mean composition (oxides, wt %) of the HaH 286 meteorite and compositions of selected eucrites

Oxide	HaH 286	Sioux County	Stannern	Nuevo Laredo	Serra de Mage	3 cumulate eucrites[##]	14 noncumulate eucrites*
SiO_2	46.38	49.2[#]	49.7[#]	49.5[#]	48.5[#]	ns	ns
MgO	5.36	6.88	6.97	5.55	10.7	6.01–8.54[##]	6.16–7.77*
FeO	16.82	18.4	17,8	19.6	14.4	15.57–19.76	18.28–21.62
S	0.10	0.07	nd	nd	0.15	nd	nd
Al_2O_3	15.19	13.1	12.3	12.2	14.8	6.86–14.77	11.19–14.41
CaO	12.32	10.4	10.7	10.3	9.75	5.87–9.80	9.99–11.12
Na_2O	0.51	0.41	0.62	0.51	0.25	0.25–0.45	0.21–0.59
Cr_2O_3	0.29	0.32	0.34	0.28	0.63	0.41–0.82	0.24–0.38
MnO	0.49	0.55	0.53	0.58	0.48	0.45–0.63	0.48–0.60
K_2O	nd	0.03	0.07	0.05	0.01	nd	nd
P_2O_5	nd	nd	0.10	nd	0.03	nd	nd
TiO_2	0.52	0.58	0.98	0.83	0.13	0.17–0.43	0.54–1.07

[#] Hutchison's data: Sioux County, Stannern, Nuevo Laredo, Serra de Mage (Hutchison, 2004).
[##], * Barrat et al., data for 17 eucrites (Barrat et al., 2000).
[##] Cumulates (3 eucrites), * noncumulates (14 eucrites). nd = not detected. ns = not specified.

of HaH 286 (0.52%, 3.1) indicates that the HaH 286 eucrite can be included into the trend line for MG-Nuevo Laredo group of eucrites. TiO_2 content in HaH 286 overlaps with both the main group (MG, with a range of 0.6–0.8 wt%) and the Nuevo Laredo groups of eucrites. Since the MG eucrites have a somewhat lower range of FeO*/MgO ratios, between 2.4 and 2.5 (Barrat et al., 2000), it is likely that HaH 286 is a member of the Nuevo Laredo group of eucrites.

Mineral Composition and Microstructure

Since the elements: Fe, Mg, Si, O, Ca, Al and Na make up over 99 percent of the meteorite by weight (Tab. 1), it is evident that the most common minerals in the meteorite are: calcium-poor pyroxene $(Mg,Fe,Ca)_2Si_2O_6$, and plagioclase feldspar (solid solution of albite $NaAlSi_3O_8$ and anorthite $CaAl_2Si_2O_8$) with a high anorthite content. Orthopyroxene $(Mg,Fe)_2Si_2O_6$ is possible. Ilmenite ($FeTiO_3$) as well as chromite ($FeCr_2O_4$) should also be present as accessory minerals.

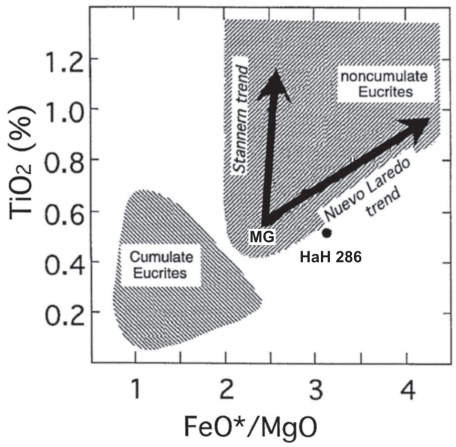

Fig. 3. TiO_2 content versus FeO*/MgO ratio for cumulate and noncumulate eucrites (Barrat et al., 2000). Data for HaH 286 (0.52 wt% of TiO_2, FeO*/MgO = 3.1) reveal that it is a noncumulate eucrite belonging to MG-Nuevo Laredo trend.
FeO* = total FeO.

Si, Mg, Fe, Ca, Al, Na and O contents prove that pyroxene and plagioclase are the dominant minerals in HaH 286. Preliminary identification of clinopyroxenes and plagioclase feldspars in the HaH 286 meteorite was done by Raman spectroscopy (Szurgot et al., 2011). Micro-Raman spectroscopy also revealed the presence of quartz crystals.

Fig. 1 shows an optical image of HaH 286 that reveals the major characteristics of the achondrite: the presence and domination of pyroxene and plagioclase crystals. X-ray maps depicting the distribution of elements and minerals and electron microscope images of HaH 286 are shown in figures 4–8.

Elemental X-ray maps of Fe, Al, Ca, Mg, Si, Cr and O together with the BSE image of the same area of meteorite are presented in Fig. 4. They show that oxygen is distributed more or less uniformly. Iron and magnesium reveal the location of pyroxene crystals and show that pyroxene is a dominant mineral. Plagioclase, is the other major mineral, as seen in the X-ray Al map. The three minerals: chromite located by chromium, silica located with silicon, and ilmenite located via the presence of black patches in the Si map, are minor minerals of the HaH 286 eucrite. Calcium denotes plagioclase, as well as two types of pyroxenes: one with a lower and the other with a higher wollastonite content.

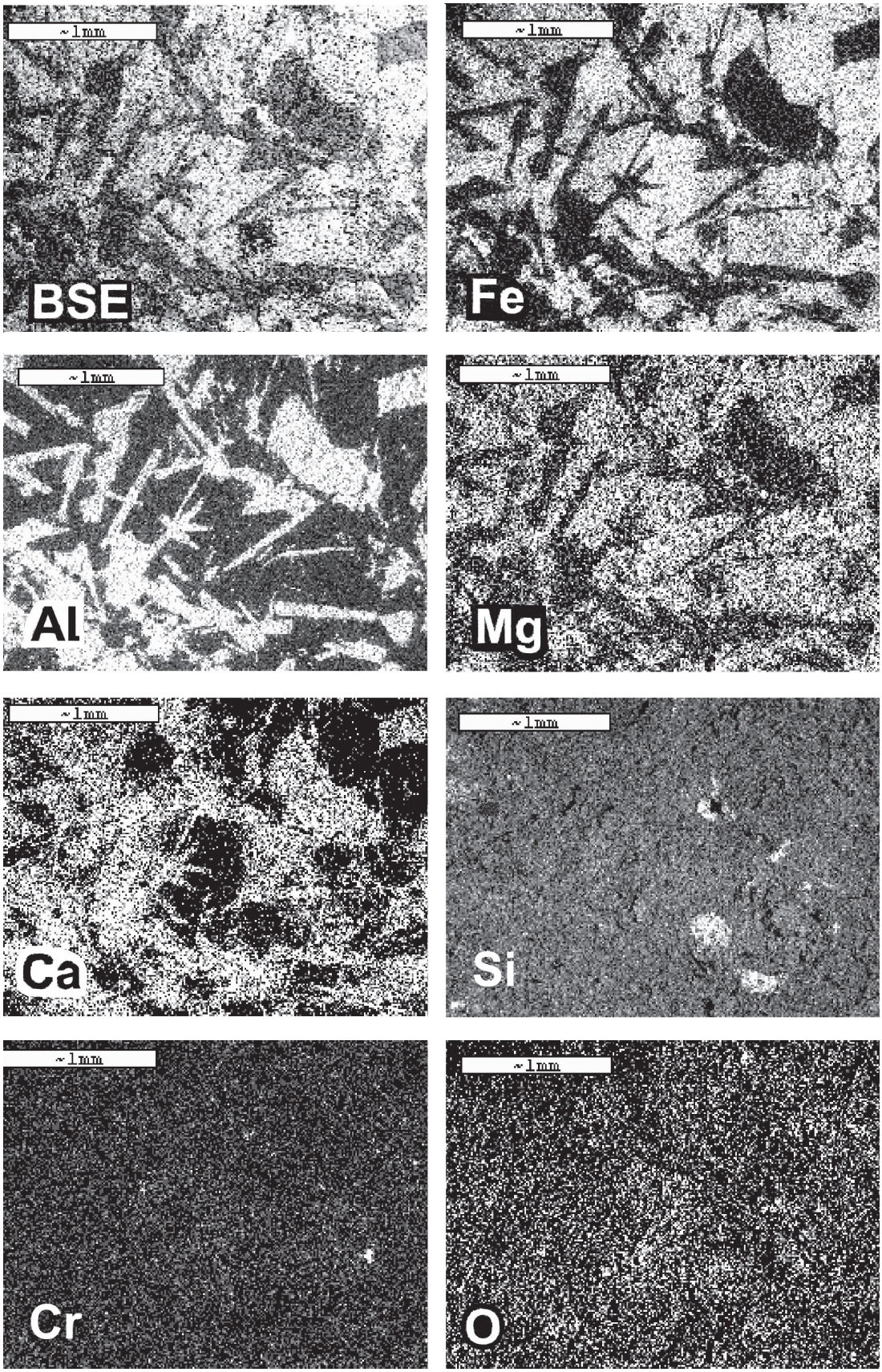

Fig. 4. Backscatter electron image (BSE) and chemical distribution maps (Fe, Al, Mg, Ca, Si, Cr and O) of the HaH 286 meteorite. Oxygen reveals silicates, oxides, and feldspars. Iron and magnesium reveal the location of pyroxene, and aluminium denotes the location of plagioclase crystals. Chromium indicates the location of chromite, and silicon shows the location of silica. Calcium is present in plagioclase and in pyroxenes (some pyroxenes have higher, and some have lower Ca contents). In each X-ray map, the higher density of white spots denotes higher abundances of given elements. Black areas mean that the element is absent

a) b)

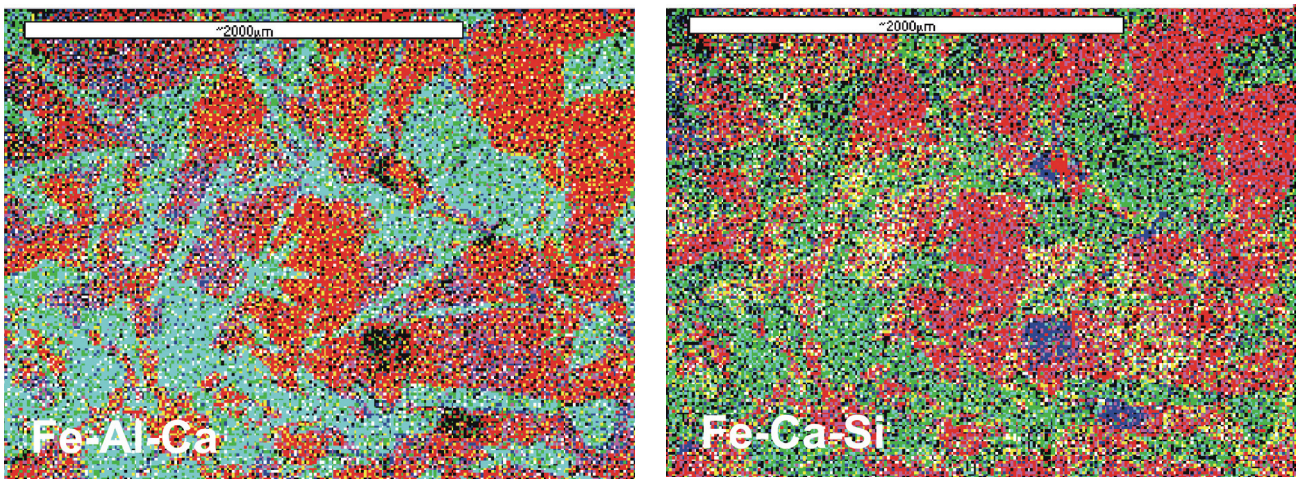

Fig. 5. Mineral maps of the same area of HaH 286 revealing major minerals. Images 5a and 5b consist of superimposed: a) Fe, Al and Ca, and b) Fe, Ca and Si elemental X-ray maps. Colour of elements: a) Fe is red, Al is green and Ca is blue, b) Fe is red, Ca is green, and Si is blue. Colour of minerals: a) pyroxene with lower Ca content is red, and pyroxene with higher Ca content is lilac, plagioclase is blue-green (cyan), and silica is black, b) pyroxene with lower Ca content is purple, and pyroxene with higher Ca content is yellow, plagioclase is green, and silica is blue

Fig. 5 shows two mineral maps of the same area of HaH 286. The images were created by superimposing X-ray maps of representative elements. The two mineral maps presented in Figs. 5a and 5b consist of superimposed: a) Fe, Al, and Ca and b) Fe, Ca and Si elemental X-ray maps. In Fig. 5a, pyroxene with lower Ca contents is red, pyroxene with higher Ca contents is lilac, plagioclase is cyan-green, and silica is black. In Fig. 5b pyroxene with lower Ca contents is purple, and pyroxene with higher Ca contents is yellow, plagioclase is green and silica is blue.

The X-ray elemental and mineral maps enabled us to estimate the modal composition of HaH 286 eucrite. According to our data, HaH 286 contains: pyroxene (54 vol%), plagioclase (44 vol%), silica (1 vol%), ilmenite (0.8 vol%), and chromite (0.1 vol%) (Tab. 4). Troilite content estimated by optical microscopy is about 0.1%. Tab. 4 shows that the modal composition of HaH 286 classifies this meteorite as a basaltic, nonocumulate eucrite (compare the mineral content of HaH 286 with the contents commonly seen in basaltic eucrites).

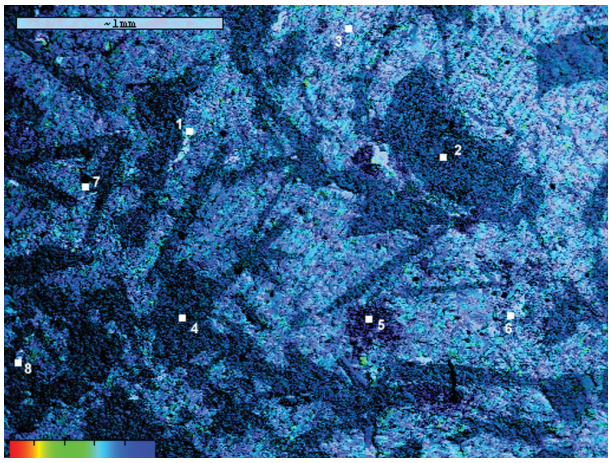

Fig. 6. X-ray Cameo image of the same region of HaH 286 as that shown in Figs 4 and 5. 1 – ilmenite, 2 – An87, 3 – En36Fs58Wo6, 4 – An94, 5 – silica, 6 – En34Fs53Wo13, 7 – En91Fs7Wo1, 8 – An90. The colour scale red-green-blue represents X-ray energy in the range between 0.2 keV (red) and 5 keV (blue). Blue represents Ca content: dark-blue means higher Ca content, and light-blue, lower Ca content. Green represents S and Si. Field of view: 3 × 2.2 mm

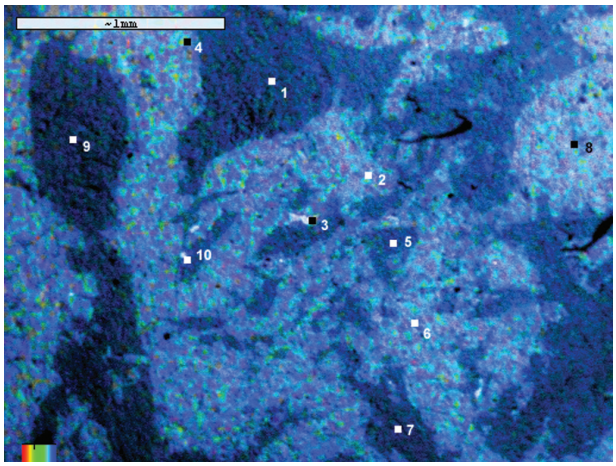

Fig. 7. X-ray Cameo image of another region of HaH 286. 1 – An90, 2 – En37Fs57Wo6, 3 – chromite and ilmenite, 4 – En35Fs62Wo3, 5 – An88, 6 – En35Fs55Wo10, 7 – An86, 8 – En34Fs62Wo4, 9 – An100, 10 – chromite and ilmenite. The colour scale red-green-blue represents X-ray energy in the range between 0.6 keV (red) and 1.75 keV (blue). In this scale, blue represents Si content, green, Mg content, and red represents Fe, Ti, and Cr content. Field of view: 3 × 2.2 mm

Table 4. Modal composition of HaH 286 and basaltic eucrites

Mineral	HaH 286	22 Eucrites (Delaney et al., 1984)	26 Eucrites (Mayne et al., 2009)	Eucrites (Hutchison, 2004)
Pyroxene	54	51.3 ± 2.6* [47.5–56.2]	49.9 ± 5.4* [38–60]	[63–50]
Plagioclase	44	43.1 ± 2.1 [39.4–46.6]	45.7 ± 6.1 [35–61]	[30–47]
Silica	1	4.0 ± 1.5 [1.1–7.7]	3.2 ± 2.7 [0–12]	[1–4.7]
Ilmenite	0.8	0.8 ± 0.3 [0.3–1.5]	ns	[tr–3.3]
Chromite	0.1	0.2 ± 0.2 [tr–0.5]	ns	[tr–0.6]
Troilite	0.1##	0.4 ± 0.3 [tr–1.1]	ns	[tr–0.5]
Fe Metal	nd	tr [tr–0.3]	ns	[tr–0.5]
Phosphate	nd	0.2 ± 0.1 [tr–0.4]	ns	[tr–0.3]
Fayalite	nd	ns	ns	[0–tr]
OSM**	1#	1.4±0.8#	0. 9 ± 0.7 [0–3]	ns

* Average of 22 eucrites (Delaney et al., 1984) and of 26 eucrites (Mayne et al., 2009) together with the standard deviation.
**OSM = oxide + sulfide + metal.
The sum of ilmenite, chromite, troilite and Fe metal, specified in upper rows as separate phases.
[ ] The range of values; nd = not detected; ns = not specified; tr = trace (< 0.1 vol%).
The modal abundance of troilite was estimated by optical microscopy. Pyroxene = orthopyroxene, pigeonite and augite.

The energy dispersive (EDS) spectra revealed (apart from the mean) the local composition of the meteorite. Pigeonite, with the compositions En36Fs58Wo6, En37Fs57Wo6, En35Fs55Wo10, En34Fs53Wo13, is commonly present in the meteorite (Figs. 6, 7). Data presented in Tab. 1 enabled us to determine the mean composition of pigeonite in the meteorite. Pigeonite's mean composition is En34Fs59Wo7, and the range of local compositions is En34–36Fs53–62Wo3–13. Data presented in Tab. 5 show that pigeonite is Fe-rich, and that its composition is characteristic of basaltic eucrites. This is seen in a pyroxene quadrilateral diagram. However, Figs 5, 6, 7 and Tab. 5 show that, apart from clinopyroxene pigeonite, orthopyroxene (En35Fs62Wo3, En34Fs62Wo4, and even En91Fs7Wo1) also occurs in the HaH 286 meteorite. The X-ray maps shown in Figs. 4 and 5 revealed two pyroxenes, one with higher wollastonite (Wo) content, and one with lower Wo content. These results suggest that the grains are clinopyroxene pigeonite (Px with higher Wo content), and orthopyroxene (Px with lower Wo content).

EDS spectra enabled us to identify and determine the composition of plagioclase in the HaH 286 meteorite. According to data presented in Tab. 1, the mean composition of the plagioclase in the meteorite is An88Ab12. Local analyses revealed that anorthite contents of plagioclase span a wide range of values from An86 to An100 (An86–100Ab14–0). Figs 6 and 7, in addition to Tab. 5, show that HaH 286's plagioclase composition is as follows: An86Ab14, An87Ab13, An88Ab12, An90Ab10, and An100Ab0. Apart from the two dominant minerals, pyroxene and plagioclase, minor minerals typical of eucrites have been revealed in HaH 286: silica, ilmenite and chromite. HaH 286 can be classified as a basaltic eucrite.

BSE images also reveal the aforementioned minerals present in this meteorite sample. White patches and veins in Fig. 8 are ilmenite and chromite, light grey areas in this BSE image are pyroxene, darker areas are plagioclase, and nearly black areas are silica, as expected for this type of meteorite. This mineral composition is consistent with the mineral composition resulted from interpretation of the X-ray maps

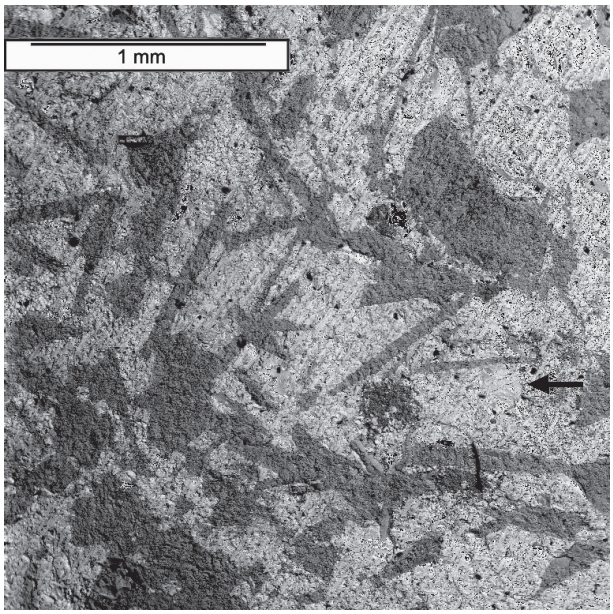

Fig. 8. BSE image of the HaH 286 eucrite revealing the constituent minerals and texture of the meteorite. Pyroxene crystals in this image are light grey and medium grey, plagioclase is dark grey, silica is black, and ilmenite and chromite are white. Arrow indicates a pigeonite crystal exhibiting compositional zoning

Table 5. Composition of plagioclases and pyroxenes in HaH 286

Mineral	HaH 286	Basaltic Eucrites (Mayne et al., 2009; McSween et al. ,2011)
Plagioclase	An88Ab12 (mean)	
	An86Ab14 An87Ab13 An88Ab12	
	An90Ab10	
	An90Ab10	
	An100	
	An86–100 (range)	An73–96
Pyroxene	En34Fs59Wo7 (mean)	
Clinopyroxene	En36Fs58Wo6	
	En37Fs57Wo6	
	En35Fs55Wo10	
	En34Fs53Wo13	
	En34–37Fs53–58Wo6–13 (range)	
Orthopyroxene	En91Fs7Wo1	
	En35Fs62Wo3	
	En34Fs62Wo4	
	En34–91Fs7–62Wo1–3 (range)	

(Figs. 4–7). HaH 286 displays a subophitic to ophitic texture consisting of lath-shaped plagioclase and anhedral, irregular pyroxene. Certain plagioclase crystals occur as radiating sprays of lath-shaped grains enclosed by larger pyroxene grains. Ilmenite occurs either as a separate phase or is associated with chromite (points 3 and 10 in Fig. 7). The coexistence of ilmenite and chromite may indicate that ilmenite was reduced to chromite. Certain pyroxenes display zonation with an exsolved texture with coarsely spaced lamellae (Fig. 8). In general, the texture of HaH 286 is typical of pyroxene-plagioclase achondrites known as eucrites (Stolper, 1977; Yamaguchi et al., 1997; Takeda, 1997; Takeda et al., 1997; Mittlefehldt et al., 1998; McSween, 1999; Norton, 2002; Hutchison, 2004; Mayne et al., 2009; McSween et al., 2011).

Fig. 8 shows laths of plagioclase crossing pigeonite and orthopyroxene crystals. The plagioclase must have grown while much of the magma was still liquid (Wasson, 1985). This structure demonstrates the origin of HaH 286 due to crystallization from a melt. This means that HaH 286 represents an igneous type rock, i.e. the rock crystallized from the magma formed by melting in the processes called partial melting, in which terrestrial and extraterrestrial basalts were created. The plagioclase crystallized from the melted material of similar composition, and their lathlike shape is the result of slow cooling (Wasson, 1985). The pyroxenes must have started to crystallize at about the same time as the plagioclase, and their equidimensional crystals ended up between the long plagioclase crystals (Wasson, 1985). HaH 286's texture can be classified as ophitic or subophitic since it resembles the texture of igneous rocks in which randomly oriented plagioclase crystals are surrounded by large pyroxene crystals. But, HaH 286 also exhibits equidimensional, coarse, anhedral plagioclase crystals coexisting with anhedral, irregular pyroxene crystals (Fig. 7). Remelting of the rock during shock collision(s) may have caused this texture. According to Grossman and Zipfel, HaH 286 is a moderately shocked meteorite, with a shock stage of S4 (Grossman & Zipfel, 2001). This indicates that HaH 286 has undergone metamorphic recrystallization, as have most HED achondrites. Impact metamorphism (breccia formation and rapid heating followed by slow cooling) led to the modification of these meteorites' original textures and mineral composition, but even highly metamorphosed eucrites have retained their initial bulk compositions (Mittlefehldt & Longhi, 1998).

An analysis of the molar ratios Fe/Mn and Fe/Mg in HaH 286 provides evidence that the meteorite belongs to the evolved achondrites rather than to the primitive achondrites. This conclusion is based on Goodrich and Delaney's results, in which they noted that primitive achondrites, exhibiting metamorphic textures appropriate for solid residues from which melts were extracted, can be readily distinguished from magmatic achondrites (SNCs, HEDs, and lunar basalts) using a diagram of molar Fe/Mn versus Fe/Mg (Goodrich & Delaney, 2000; McSween & Huss, 2010). The diagram is shown in Fig. 9. Primi-

tive achondrites have Mn/Mg ratios distinctly different from evolved, magmatic achondrites, and the Mn/Mg ratio of magma can change during the process of fractional crystallization (Goodrich & Delaney, 2000; McSween & Huss, 2010). The evolved achondrites exhibit a nearly constant Fe/Mn ratio. In Fig. 9, the PA trend line represents data for primitive achondrites (lodranites, acapulcoites, winonaites, brachinites, and ureilites), and the MA trend line (with the small slope) represents data for evolved, magmatic achondrites (HEDs and SNCs). The field of magmatic achondrites is marked as the area between the two dashed lines. Figure 9 shows that the experimental point (Fe/Mn = 34, Fe/Mg = 1.75) representing HaH 286 meteorite is located within the field of magmatic HED achondrites (the lunar basalt field located above the HED field is not drawn here).

The Fe/Mn ratio in pyroxenes is diagnostic for determining a common planetary origin of meteorites, as the primordial values of these elements are believed to remain constant through planetary differentiation (Papike, 1998; Papike et al., 2003; Mayne et al., 2009). Recent data on Fe/Mn – Fe/Mg relations for twenty-nine unbrecciated eucrites show that it is possible to distinguish between cumulate and noncumulate eucrites (Mayne et al., 2009). Our data for HaH 286 indicate that this achondrite belongs to the noncumulate eucrites since HaH 286 (shown in Fig. 9) is located within the field of noncumulates.

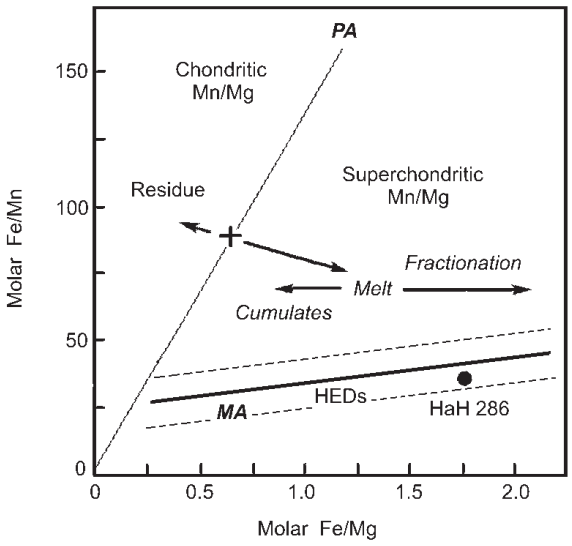

Fig. 9. Diagram used to distinguish between achondrites crystallizing from melts (evolved achondrites) and primitive achondrites, representing the solid residue from extracted melt (Goodrich & Delaney, 2000; McSween & Huss, 2010). Line MA represents the trend for magmatic, evolved achondrites, and line PA represents the trend for primitive achondrites. Notice that the experimental point (filled circle) for the HaH 286 achondrite (Fe/Mn = 34, Fe/Mg = 1.75) is located within the field of magmatic achondrites

Table 6. Thermophysical properties of HaH 286

Property	HaH 286 value
Specific heat capacity (Szurgot, 2003)	657 J kg^{-1} K^{-1}
Thermal conductivity (Szurgot, 2011b)	1.9 W m^{-1} K^{-1}
Thermal diffusivity (Szurgot & Wojtatowicz, 2011)	$0.93 \cdot 10^{-6}$ m^2 s^{-1}
Bulk density (Szurgot, 2003)	3.13 g cm^{-3}

Physical properties of HaH 286

In Tab. 6, data on bulk density and thermophysical properties of HaH meteorite have been compiled (Szurgot, 2003, 2011a,b; Szurgot & Wojtatowicz, 2011). They show that the bulk density, specific heat capacity, thermal diffusivity and thermal conductivity of HaH 286 are characteristic of a basalt.

CONCLUSION

All identified minerals are characteristic of eucrites. Elemental, oxide and modal composition data and microstructure, indicate that the HaH 286 meteorite is a pyroxene-plagioclase basaltic achondrite, one of the non-cumulate eucrites.

ACKNOWLEDGEMENTS

We would like to express our gratitude to Professor Tadeusz Przylibski for the valuable comments on the manuscript and encouragement, and also to the anonymous reviewers for their valuable suggestions and comments.

REFERENCES

Barrat J.A., Blichert-Toft J., Gillet PH., Keller F., 2000 – The differentiation of eucrites: the role of in-situ crystallization, *Meteoritics & Planetary Science*, 35, 1087–1100.

Delaney J.S., Prinz M., Takeda H., 1984 – The polymict eucrites. *Journal of Geophysical Research*, 89, *Supplement,* C251––C288.

Goodrich C.A., Delaney J.S., 2000 – Fe/Mg-Fe/Mn relations of meteorites and primary heterogeneity of primitive achondrite parent bodies. *Geochimica et Cosmochimica Acta*, 64, 149–160.

Grossman J.N., Zipfel J., 2001 - Meteoritical Bulletin, no 85, 2001 September. *Meteoritics & Planetary Science*, 36, A293––A322.

Hutchison R., 2004 – Meteorites: A petrologic, chemical and isotopic synthesis. Cambridge University Press, Cambridge, UK.

Johum K.P., Grais K.I., Hintenberger H., 1980 – Chemical composition and classification of 19 Yamato meteorites. *Meteoritics*, 15, 31–39.

Mason B., Jarosevich E., Nelen J.A., 1979 – The pyroxene-plagioclase achondrites. *Smithsonian Contributions to the Earth Sciences*, 22, 27–45.

Mayne R.G., McSween H.Y., McCoy T.J., Gale A., 2009 – Petrology of the unbrecciated eucrites. *Geochimica et Cosmochimica Acta*, 73, 794–819.

McSween H.Y., Jr., 1999 – Meteorites and their parent planets. Cambridge University Press, Cambridge, UK.

McSween H.Y., Jr., Huss G.R., 2010 – Cosmochemistry. Cambridge University Press, Cambridge, UK.

McSween Jr. H.Y., Mittlefehldt D.W., Beck A.W., Mayne R.G., McCoy T.J., 2011 – HED meteorites and their relationship to the geology of Vesta and the Dawn mission. *Space Science Reviews*, 163, 141–174.

Mittlefehldt D.W., Longhi J. 1997 – Basaltic achondrite meteorites, [in:] Shirley J.H., Fairbridge H. (eds), *Encyclopedia of Planetary Sciences*, Chapman & Hall, London, 65–68.

Mittlefehldt D.W., McCoy T.J., Goodrich C.A, Kracher A., 1998 – Non-chondritic meteorites from asteroidal bodies, [in:] Papike J.J. (ed.), *Planetary materials,* Mineralogical Soc. America, Washington, 4.1–4.195.

Norton O.R., 2002 – The Cambridge encyclopedia of meteorites. Cambridge University Press, Cambridge, UK.

Papike J.J, 1998 – Comparative planetary mineralogy: chemistry of melt-derived pyroxene, feldspar, and olivine, [in:] Papike J.J. (ed.), *Planetary materials,* Mineralogical Soc. America, Washington, 7.1–7.11.

Polański K., 2008 – Analytical electron microscopy in crystals investigations, [in:] Wojtczak L. and Ziomek J. (eds), *Crystals in nature and technology,* University of Lodz, Łódź, 173–190 (in Polish).

Reed S.J.B., 2000 – Electron microprobe analysis and scanning electron microscopy in geology, Cambridge University Press, Cambridge, UK.

Stolper E., 1977 – Experimental petrology of eucritic meteorites. *Geochimica et Cosmochimica Acta*, 41, 587–611.

Szurgot M., 2003 – Thermophysical properties of meteorites, Specific heat capacity. *2nd Meteorite Seminar in Olsztyn*, 136–145 (in Polish).

Szurgot M., 2011a – On the specific heat capacity and thermal capacity of meteorites. *42nd Lunar and Planetary Science Conference,* Abstract #1150.pdf

Szurgot M., 2011b – Thermal conductivity of meteorites. *Meteoritics & Planetary Science*, 46, *Supplement*, A230.

Szurgot M., Wojtatowicz, T.W., 2011 – Thermal diffusivity of meteorites. *Meteoritics & Planetary Science*, 46, *Supplement,* A230.

Szurgot M., Tomasik A., Kozanecki M., 2011 – Identification of minerals in HaH 286 eucrite by Raman spectroscopy. *53rd Polish Crystallographic Meeteing in Wrocław,* 278–279 (in Polish).

Takeda H., 1997 – Mineralogical records of early planetary processes on the howardite, eucrite, diogenite parent body with reference to Vesta. *Meteoritics & Planetary Science*, 32, 841–853.

Takeda H., Ishi T., Arai T., Miyamoto M., 1997 – Mineralogy of the Asuka 87 and 88 eucrites and crustal evolution of the HED parent body. *Antarctic Meteorite Research*, 10, 401–413.

Wasson J.T, 1985 – Meteorites, their record of early solar-system history. Freeman and Comp., New York, USA.

Yamaguchi A., Taylor G.J., Keil K., 1997 – Shock and thermal history of equilibrated eucrites from Antarctica. *Antarctic Meteorite Research*, 10, 415–436.

Yamaguchi A., Barrat J.A., Greenwood R.C., Shirai N., Okamoto C., Setoyanagi T., Ebihara M., Franchi I.A., Bohn M., 2009 – Crustial partial melting on Vesta: evidence from highly metamorphosed eucrites. *Geochimica et Cosmochimica Acta*, 73, 7162–7182.

Publishers: Wrocław University of Technology, Faculty of Geoengineering, Mining and Geology
Polish Meteorite Society